

Oct 18th, 12:00 AM

Axial Load Capacity of Sheeted C and Z Members

Richard C. Kaehler

James M. Fisher

Neil J. Glaser

Follow this and additional works at: <https://scholarsmine.mst.edu/isccss>



Part of the [Structural Engineering Commons](#)

Recommended Citation

Kaehler, Richard C.; Fisher, James M.; and Glaser, Neil J., "Axial Load Capacity of Sheeted C and Z Members" (1994). *International Specialty Conference on Cold-Formed Steel Structures*. 3.
<https://scholarsmine.mst.edu/isccss/12iccfss/12iccfss-session8/3>

This Article - Conference proceedings is brought to you for free and open access by Scholars' Mine. It has been accepted for inclusion in International Specialty Conference on Cold-Formed Steel Structures by an authorized administrator of Scholars' Mine. This work is protected by U. S. Copyright Law. Unauthorized use including reproduction for redistribution requires the permission of the copyright holder. For more information, please contact scholarsmine@mst.edu.

AXIAL LOAD CAPACITY OF SHEETED C AND Z MEMBERS

by Neil Glaser¹, Richard Kaehler² and James Fisher³

SUMMARY

An equation is developed for calculating the axial load capacity of C and Z shaped members used in roof or wall systems. The equations were determined to be valid for through fastened metal decking but not standing seam roof decking.

INTRODUCTION

Sheeted Cold-Formed C and Z members are often used in wind, seismic and stability bracing systems in metal buildings. They typically function as compression struts in a horizontal "truss" system. A metal roof which is either through fastened (screw down) or a standing seam roof system with fixed or sliding clips is attached to one flange of the C or Z sections. The C and Z members must resist bending moments as well as the axial loads from wind, seismic, or stability forces.

The purpose of this research reported herein was three fold:

1. To develop a simple equation for the calculation of the axial load capacity for C and Z members with one flange attached to a through fastened metal roof or wall panel.
2. To determine if the axial load capacity is dependent on whether the member is simple-span or continuous.
3. To determine if the simple equation developed for a through fastened roof or wall panel can be used to predict the axial load capacity for purlins with standing seam roofs.

BACKGROUND

The capacity of strut purlins was previously investigated by Hatch et al (1991). The researchers concluded that:

- "1. The AISI interaction equation provides conservative but reasonable results with respect to predicting the ultimate failure strength of diaphragm braced strut-purlins subject to combined axial and uplift loading.
2. Simaan's method of determining axial capacity of diaphragm braced cold-formed sections is general enough to be applicable to strut-purlins in metal building roof systems.

¹Engineer, Computerized Structural Design, Inc.

²Vice President, Computerized Structural Design, Inc.

³Vice President, Computerized Structural Design, Inc.

3. The axial capacity of diaphragm braced strut-purlins is significantly influenced by the location of the purlin to deck fastener.
4. The uplift capacity of the purlin and decking system can be limited by the fastener pull through strength of the deck."

ANALYTICAL INVESTIGATION

The Simaan method (Simaan, 1973) and the axial load tests reported in the Hatch research served as the basis for the development of a simple equation for the axial load capacity of C's and Z's with one flange connected to a through fastened roof or wall panel.

A parametric study was conducted using the variables required in the Simaan equations. These are:

1. Member Length.
2. Section Depth.
3. Flange Width.
4. Member Thickness.
5. Rotational Stiffness of the Deck to Flange Connection.
6. Form Factor (Q).
7. Allowable Diaphragm Strain.
8. Diaphragm Shear Rigidity.
9. Allowable Purlin Rotation.
10. Yield Stress.
11. Fastener Spacing.

Phase I:

The parametric study consisted of two phases. In phase one all of the listed variables were studied using a computer program which implements the Simaan equations to determine which variables could possibly be eliminated in a simplified equation. The variables were evaluated in the Simaan equations using data for 7 inch to 10 inch deep C and Z sections.

It was determined that, section depth, flange width, member thickness, and the rotational stiffness of the deck to flange connection could not be eliminated from the equation; however the remaining variables could be ignored provided certain practical limitations are imposed. A summary of the findings from Phase I are discussed below:

Form Factor Q - The Simaan work was conducted when the American Iron and Steel Institute Specification (1968) used a form factor for the calculation of axial capacity of cold-formed columns. For the members studied, form factors are nearly equal to one since the buckling stress is quite low. The parametric study indicated that for form factors greater than 0.5 the critical stress did not change, and thus Q could be neglected in the formulation of a simplified equation. The critical stress can thus be determined using the gross area of the section.

Allowable Diaphragm Strain - The allowable diaphragm strain is determined as the deflection of the diaphragm at eight tenths of the ultimate load capacity divided by the distance a. See Fig. 1. The allowable diaphragm strain has negligible effect on the critical stress if the allowable strain is more than .002 in./in. Through fastened metal roof diaphragms generally meet this provision.

Diaphragm Shear Rigidity - The shear rigidity for use in the Simaan equations is determined from the diaphragm shear stiffness. Referring to Fig. 1, the shear stiffness, G' is defined as:

$$G' = .8P_{ult}(a) / (\Delta_d)(b), \text{ and} \quad (1)$$

$$\text{Shear rigidity} = (0.67)(G')(w), \quad (2)$$

where:

w = the width of deck contributing to the lateral support of one purlin.
 $\Delta_d = \Delta @ 0.8P_{ult}$

The parametric study indicated that the variation in shear rigidity has negligible effect on the critical stress so long as a minimum rigidity of approximately 500 kips/in./in. exists. Most through fastened metal panels meet this requirement.

Allowable Purlin Rotation - The allowable purlin rotation is defined by Simaan as ϕ_d . It is limited by the connection strength between the panel and the purlin. For large angles:

$$\phi_d = \sin^{-1} (\Delta/L), \quad (3)$$

where:

Δ = the lateral deflection of the loaded purlin flange at $0.8 M_{ult}$.
 L = the depth of the purlin web.

Based on the test data from Hatch (1991), ϕ_d varied from approximately 0.2 to 0.3 radians for 7 to 10 inch deep purlins. For this range of allowable purlin rotation, only a small variation in critical stress occurred.

Yield Stress - No effect on the critical stress resulted from varying the yield stress from 33 to 60 ksi. This would be expected since, for the sections used in the study, the critical axial compressive stress based on the Simaan equations stress varied from 12 to 20 ksi, indicating an elastic buckling failure.

Fastener Spacing - Examination of fastener spacing showed that the same critical stress level was obtained for different fastener spacings. Fastener spacings examined varied from 6 inches to 36 inches. The Simaan method assumes that the same total rotational and diaphragm stiffness and strength are achieved, regardless of fastener spacing. Previous testing was limited to typical fasteners spacings of about 12 inches.

Phase II

Phase II consisted of examining the remaining variables of:

1. Member Length
2. Section Depth
3. Flange Width
4. Member Thickness
5. Rotational Stiffness of the Deck to Flange Connection.

Each of these variables was investigated by examining its influence on the critical buckling stress as predicted by the Simaan equations. In order to reduce the number of variables, only values which are typical of strut purlins as commonly used in the metal building industry were studied. Lengths of 15 to 30 feet were examined for the 28 typical sections

shown in Table 1. The typical sections were arrived at by examining sections produced by several metal building manufacturers.

The parameters from Phase I which were shown to have a negligible influence on the critical buckling stress were held constant for Phase II. The constants were:

Yield Strength	= 55 ksi
Form Factor	= 1.0
Fastener Spacing	= 12 inches
Diaphragm Shear Rigidity	= 656 kips/in/in
Allowable Diaphragm Strain	= .0035 in/in
Allowable Purlin Rotation	= .2588 radians

These are the same values used in the Hatch report.

Member Length - The buckling stress predicted by the Simaan equations is a function of member length. For short to intermediate lengths, the buckling behavior is similar in nature to the buckling behavior of a plate subjected to axial stress. At failure a plate will buckle into one or more sinusoidal waves. Shown in Fig. 2 is a plot of critical stress versus aspect ratio for a plate. The same lower bound on critical stress exists for each mode; however if the section is slightly longer or slightly shorter than the exact length which permits an integer mode then an increase in critical stress occurs. A similar behavior illustrated in Fig. 3, was noted and studied using the 28 typical strut sections. It was concluded that the critical stress should be based on the lower bound critical stress for lengths typically encountered, i.e. spans up to 33 feet. Thus, for the equation formulation presented, member length is not a parameter in the equation. This approach can in a few cases result in up to a 25 percent conservative estimate of the actual buckling stress. This conservatism is illustrated in Fig. 3. It should be noted that strong axis buckling will control at longer lengths.

Rotational Stiffness of the Deck to Flange Connection - The rotational stiffness of the connection has a large impact on the critical stress. It is a function of several parameters, the most influential of which are the location of the fastener on the flange of the C or Z section, panel thickness, section thickness, and fastener type. Values for the rotational stiffness of the deck to flange connection are obtained through testing. The input values for the Simaan equations can be obtained from test data using the AISI (1989) test for "Rotational-Lateral Stiffness Test Method for Beam-To-Panel Assemblies". **For input into the Simaan equations, the test values must be multiplied by the depth of the section squared.** Values used in this study were obtained from the Hatch report. Hatch tested various fastener locations on C and Z sections. These locations were described as strong, medium and weak. The strong values were those where the fastener was located the farthest from the Z section web, the medium values were those where the fastener was located approximately in the middle of the flange, and the weak values were those where the fastener was located close to the Z section web.

A plot of the Hatch rotational stiffness data is shown in Fig. 4. The data shows the relationship between the rotational stiffness of the deck to flange connection and section thickness for the three different fastener locations, strong, medium and weak. A best fit linear equation was determined for each of the three fastener placement locations (strong, medium and weak). For the weak fastener location there are two values that do not fit in well with the other four values. These two values were neglected when determining the equation for the weak fastener placement location. Equations 4, 5 and 6 represent the

results of the best fit equations. These equations assume that a five foot width of diaphragm is tributary to each member.

$$\text{Weak (fastener close to web)} \quad F = 0.72t - .012 \quad (4)$$

$$\text{Medium (fastener at mid flange)} \quad F = 2.02t - .035 \quad (5)$$

$$\text{Strong (fastener close to stiffener lip)} \quad F = 2.51t - .043 \quad (6)$$

where:

F = Rotational stiffness of deck to flange connection (k-in/in-rad)

t = Strut section thickness (in).

The three equations were then combined to form a generalized equation:

$$F = (2.51t - .043)(1.04x + .15) \quad (7)$$

where:

x = The fastener distance from web divided by the flange width.

Equation (7) was based on x values of .15, .57, and .85 for weak, medium, and strong fastener locations respectively. These were the typical values provided in the Hatch Report.

Depth, Flange Width, and Section Thickness - Depth, flange width, and section thickness all have a significant effect on the critical stress. To determine the interrelationship of these parameters on the critical stress, three dimensional plots of critical stress versus depth and flange width were made for each combination of thickness and fastener placement. All of the plots could be closely approximated by a plane. Linear regression analysis was used to obtain an equation for each plane. Twelve equations were obtained, three for each thickness, as given below:

For t = 0.060":

$$\text{Strong} \quad \sigma = 3b - 3.25h + 36.5 \quad (8)$$

$$\text{Medium} \quad \sigma = 3b - 2.75h + 29.5 \quad (9)$$

$$\text{Weak} \quad \sigma = 1.5b - 1.75h + 19.75 \quad (10)$$

For t = 0.075":

$$\text{Strong} \quad \sigma = 3b - 1.88h + 26.5 \quad (11)$$

$$\text{Medium} \quad \sigma = 2.5b - 1.63h + 22.75 \quad (12)$$

$$\text{Weak} \quad \sigma = 2b - 1.13h + 14.0 \quad (13)$$

For t = 0.105":

$$\text{Strong} \quad \sigma = 3b - 2h + 28.5 \quad (14)$$

$$\text{Medium} \quad \sigma = 2.5b - 1.63h + 23.75 \quad (15)$$

$$\text{Weak} \quad \sigma = 1.5b - 1.13h + 16.25 \quad (16)$$

For t = 0.120":

$$\text{Strong} \quad \sigma = 3.5b - 1.75h + 24.2 \quad (17)$$

$$\text{Medium} \quad \sigma = 2.5b - 1.50h + 22.2 \quad (18)$$

$$\text{Weak} \quad \sigma = 2.0b - 1.25h + 16.0 \quad (19)$$

where:

σ = Critical Stress (ksi),

b = Flange width (in),

h = Section depth (in).

The Generalized Equation: The twelve equations generated for varying depth and flange width for each Z section thickness were combined into three equations by incorporating the section thickness as a variable.

For the strong fastener location: $\sigma = (.89t + 0.90)(3b - 2h + 28.5)$ (20)

For the medium fastener location: $\sigma = (1.17t + 0.93)(2.5b - 1.63h + 22.75)$ (21)

For the weak fastener location: $\sigma = (1.47t + 0.83)(1.5b - 1.13h + 16.25)$ (22)

where:

t = Strut section thickness (in).

The location of the fastener was then incorporated into equations 20, 21 and 22 to obtain one equation for the critical buckling stress.

$$\sigma = (0.79x + 0.54)(1.17t + 0.93)(2.5b - 1.63h + 22.8) \quad (23)$$

The generalized equation was compared to the Hatch Report test values and to values obtained from the Simaan equations. The comparison with the lower bound values, estimated from the length versus critical stress plots obtained from Simaan's program, demonstrated a very close relationship (See Figs. 5-7). For these three figures the Section No. corresponds to the section numbers shown in Table 1. Section numbers 1 to 4 are 6" sections, 5 to 13 are 8" sections, 14 to 22 are 10" sections and 23 to 28 are 12" sections.

For the weak fastener locations, the equation provides results that are generally within 1 ksi of the Simaan values. The values are slightly unconservative with the exception of the 6" Z sections.

The values obtained from Equation (23), for the medium fastener locations, are almost identical to the Simaan values. Again the values are slightly unconservative with the exception of the 6" Z sections, which are on the conservative side.

For the strong fastener locations, the equation again provides results that are within 1 ksi of the Simaan values. Similar to the results for the weak fastener locations, the values are slightly unconservative with the exception of the 6" Z sections.

Equation (23) also compares favorable to the Hatch test values for axially loaded Z shaped strut purlins (See Fig. 8). The results also show that the Equation (23) is as good an estimate of critical stress as Simaan's equations. Also shown in Table 2 is a comparison between the Hatch test values and values calculated using Equation 23. The calculated values using both the Simaan procedures and Equation 23 are in good agreement with the test values. Based on the mean values and the coefficient of variations it can be seen that Equation 23 is as good of a prediction as the Simaan procedure for the purlins tested by Hatch et al.

Since Z and C sections behave similarly relative to their critical axial stress, it was decided that Equation (23) could probably be used for C sections by simply redefining the value of (x). Fastener placements are opposite for C versus Z sections, i.e. the strong location for a Z section is the weak location for a C section and vice versa. Defining x as (Flange width - Fastener distance from the web) divided by flange width, Equation (23) was checked against the same sections from Table I except that property values for C sections were used, with appropriate changes being made in the values if I_y , I_{xy} , X_o and C_w . Illustrated in Figs. 9 to

10 are the comparisons between the Equation (23) and Simaan's Equation. Good correlation was obtained.

Equation (23) was also compared to test values for C shapes in the Hatch report. This comparison is shown in Fig. 12.

Summary of the Analytical Investigation:

The ultimate axial load capacity for a C or Z section with a diaphragm panel attached to one flange can be determined by multiplying the critical stress obtained from equation 23 times the full (gross) area of the section.

$$P_u = (0.79x + 0.54)(1.17t + 0.93)(2.5b - 1.63h + 22.8) A \quad (24)$$

where:

- P_u = The required axial strength
- x = The fastener distance from the web centerline divided by the flange width for Z sections, and
- x = (the flange width - the fastener distance from the web centerline) divided by the flange width for C sections.
- t = The section thickness, inches
- b = The flange width, inches
- h = The section depth, inches
- A = The full unreduced cross-sectional area at the member

EXPERIMENTAL INVESTIGATION

Six full scale tests were originally planned to investigate the second and third purposes of the research. The test program was as follows:

One test was to serve as a base test. This test consisted of two twenty-five foot long opposed Z sections with a twenty-six gage screw down panel (typical profile of 1-1/2 " deep major corrugations spaced at 12" o.c.) connected to one of the flanges of each section.

To determine whether or not the axial load capacity was dependent on purlin continuity, a two span system was tested. The two spans were each 25 foot in length with laps of 2'-0" on each side of the center support. The same size Z sections as in the base test were used.

Four simple span tests with standing seam roofs were conducted. Two different types of standing roofs were tested. Both types were 24 inch wide, trapezoidal rib, but one had seamed laps whereas the other had a "snap-on" lap. The panel clips also differed in construction and stiffness. Two identical tests of each type were to be tested and compared to the base test.

All test Z sections were 8 inches deep with a nominal thickness of .075 inches.

DESCRIPTION AND SUMMARY OF TESTS

A summary of the failure load for each test is shown in Table 2. Test 1 configuration is shown in Fig. 13. The 26 gage roof deck was attached to the purlins with self drilling

screws 12 inches on center. Load was applied with the hydraulic ram, spreader beams, and loading rod as shown in Fig. 13. An ultimate load of 60 kips was obtained. This is equivalent to an axial stress of 26.4 ksi in each of the Z sections. This stress significantly exceeds the predicted axial stress of 15.9 ksi from Equation (24). The failure mode appeared to be a combined strong axis and lateral torsional buckling failure. The discrepancy between the predicted failure stress and experimentally obtained failure stress was investigated by performing a second order analysis on the Z section column. It was determined that due to the initial downward camber of the test specimens of 0.5 inches, significant secondary moments were created in the system causing tensile stresses in the unsupported flange. These secondary stresses increased the apparent buckling strength of the system. It was decided that Test 1 should be repeated and that the test arrangement must be configured so that secondary tensile stresses are not generated in the unsupported flange.

Even though Test 1 was not used as the base test it did demonstrate the significance of small eccentricities in the behavior of Z and C sections subjected to axial loading. Test 1 was repeated as Test 6.

Tests 2 through 6 were also assembled as shown in Fig. 13. Test 7, the two span test, was assembled as shown in Fig. 14. As previously mentioned each test consisted of two opposed Z purlins loaded through their centroids using spreader beams and a loading rod. For the simple span tests, one end was allowed to roll in the direction of loading. For the two span test, the center support was held in place, and the both ends were allowed to roll toward the center. All of the Z sections were of the same size, and all were fabricated from the same coil. The average yield strength of the sections was 60,300 psi and the average tensile strength was 80,300 psi. These values were obtained from three different sections. Since failure stresses were well below yield, it was not necessary to obtain yield and tensile data for each failed specimen.

Prior to testing, camber and sweep data were recorded for each test assembly. In addition, the eccentricity of load relative to the purlin centroid was recorded. Dial gage readings to determine vertical deflections were taken over each support and at midspan. Load and deflection readings were recorded at 3 kip load increments.

Test 2 was conducted upside down, i.e. with the deck down, so that the initial camber would be directed in a manner so that secondary tensile stresses would not be created in the unsupported flange. The specimen was turned upside down after assembly because the negative camber was not noticed until after the initial assembly was completed. All other tests were fabricated with the camber up, and tested with the deck up.

Test data can be found in Glaser et al (1993).

OBSERVATIONS:

1. All of the Z sections rotated a considerable amount prior to failure.
2. All final failure modes consisted of a local buckle involving the stiffener lip, flange, and flange to web juncture.
3. The tests with the standing seam roof first exhibited a diaphragm failure allowing the purlins to sweep and bow horizontally. This was followed by the local buckle condition. Failure loads were considerably lower than the screw down panel test.

CONCLUSIONS AND RECOMMENDATIONS

1. Equation (24) can be used with good accuracy in lieu of the Simaan equations to predict the ultimate axial load capacity (weak axis mode) of simple span or continuous span C and Z sections attached to a diaphragm on one flange. The axial load capacity (weak axis failure mode) can be obtained by multiplying the critical stress obtained from equation (23) times the gross area of the section.

Due to the parameters investigated, the Equation is limited to the following :

- a. C and Z sections with depths of 6 to 12 inches.
 - b. Span length not exceeding 33 feet.
 - c. Roof or wall panels with fasteners spaced 12 inches on center or less, and having a minimum rotational-lateral stiffness of .0015 (fastener at mid-flange width) as determined by the AISI test procedure.
 - d. Minimum yield point of 33 ksi.
 - e. C and Z thicknesses not exceeding 0.125 inches.
2. A factor of safety of 1.92 is recommended.
 3. Strong axis strength must be checked to determine that it does not control.
 4. Equation (24) cannot be used to calculate the axial load capacity for C and Z sections with a standing seam panel attached to one flange.
 5. It is unlikely that an equation similar to equation (24) can be developed for struts braced by standing seam roofs because the strut strength is dependent on the diaphragm strength and stiffness. The diaphragm strength and stiffness variation varies dramatically between various types of standing seam roofs.
 6. The capacity of C and Z sections with standing seam panels can be obtained experimentally by obtaining the critical axial stress for the thickest section of any given depth series. The weak axis load capacity may then be calculated using the smaller value of this stress or the stress obtained from Equation (23) for any section with the same depth and flange width.

References:

Glaser, Neil J., Kaehler, Richard C., Fisher, James M., "Axial Load Capacity of Sheeted Cold-Formed C and Z Members". (1993) Report CF 93-2, American Iron and Steel Institute, Washington, D.C.

Hatch, J., Easterling, W.S., Murray, T.M., "Strength Evaluation of Strut-Purlins". (1991) Report No. CE/VPI-ST90/08, Virginia Polytechnic Institute and State University, Blacksburg, VA.

Simaan, A. (1973). "Buckling of Diaphragm-Braced Columns of Unsymmetrical Sections and Application to Wall Studs Design." Report No. 353, Department of Structural Engineering, Cornell University, Ithaca, N.Y.

"Specification for the Design of Cold-Formed Steel Structural Members", 1968, American Iron and Steel Institute, Washington, D.C.

Test procedures for use with the August 19, 1986, Edition of the "Specification for the Design of Cold-Formed Steel Structural Members", Cold-Formed Steel Design Manual - Part VII, American Iron and Steel Institute, Washington, D.C.

Section No.	Depth (inches)	Flange Width (inches)	Lip Length (inches)	Thickness (inches)
1	6	2.5	.625	.060
2	6	2.5	.625	.075
3	6	3.0	.75	.060
4	6	3.0	.75	.075
5	8	2.5	.625	.060
6	8	2.5	.625	.075
7	8	2.5	.625	.105
8	8	3.0	.75	.060
9	8	3.0	.75	.075
10	8	3.0	.75	.105
11	8	3.5	1.0	.060
12	8	3.5	1.0	.075
13	8	3.5	1.0	.105
14	10	2.5	.625	.075
15	10	2.5	.625	.105
16	10	2.5	.625	.120
17	10	3.0	.75	0.75
18	10	3.0	.75	.105
19	10	3.0	.75	.120
20	10	3.5	1.0	.075
21	10	3.5	1.0	.105
22	10	3.5	1.0	.120
23	12	3.0	.75	.075
24	12	3.0	.75	.105
25	12	3.0	.75	.120
26	12	3.5	1.0	.075
27	12	3.5	1.0	.105
28	12	3.5	1.0	.120

TABLE 1 - TYPICAL SECTIONS

Hatch Test Description	Tested Capacity	Analytical Simaan	Analytical Eq. 23	Test/Simaan	Test/Eq. 23
SP-7C-12-1	13.6	14.6	15.3	1.074	1.125
SP-7C-12-2	14.4	17.4	16.7	1.208	1.160
SP-7C-12-3	14.4	15.8	15.4	1.097	1.069
SP-10C-12-1	14.2	13.5	14.0	0.951	0.986
SP-10C-12-2	13.9	13.0	14.2	0.935	1.022
SP-10C-0	17.9	12.3	14.1	0.687	0.788
SP-10Z-12-1	13.5	15.1	15.4	1.119	1.141
SP-10Z-12-2	12.7	13.1	12.9	1.031	1.016
SP-10Z-12-3	17.3	16.3	17.1	0.942	0.988
SP-10Z-0	15.9	16.2	14.2	1.019	0.893
			Mean	1.006	1.019
			COV	14.1%	11.3%

TABLE 2 - COMPARISON OF TEST VALUES VS. ANALYTICAL VALUES

Test No.	Type	Total Failure Load (2 struts)
1	Screw Down Roof	60.0 kips
2	Standing Seam, Seamed Panel	38.0 kips
3	Standing Seam, Seamed Panel	37.2 kips
4	Standing Seam, Snap Panel	29.0 kips
5	Standing Seam, Snap Panel	26.6 kips
6	Base Test, Screw Down Roof	48.0 kips
7	Two Span, Screw Down Roof	50.3 kips

TABLE 3 - TEST DESCRIPTIONS AND FAILURE LOADS

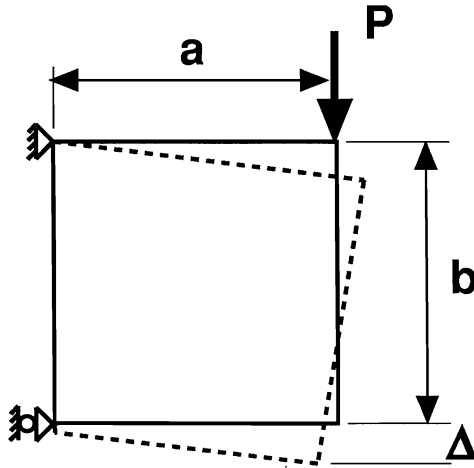


Fig. 1 Diaphragm Displacements

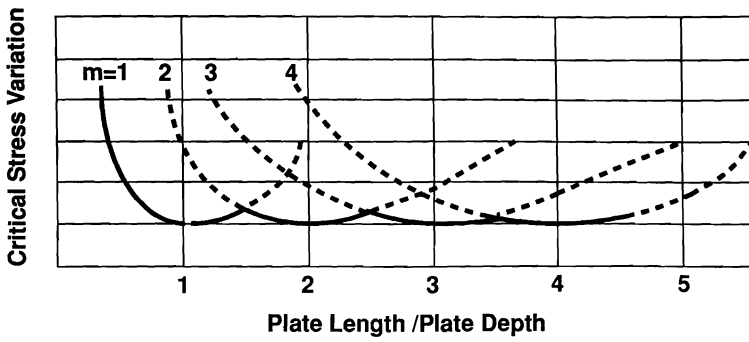


Fig. 2 Plate Buckling Modes

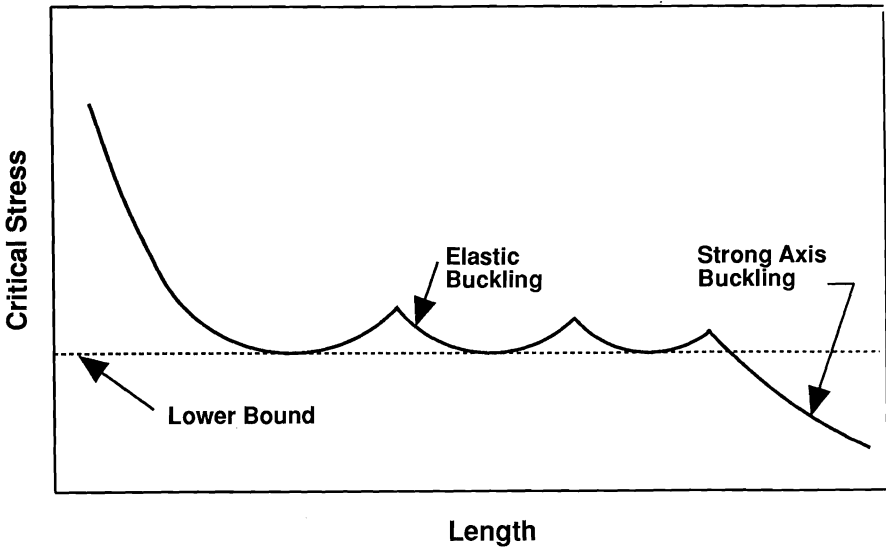


Fig. 3 Length vs. Critical Stress

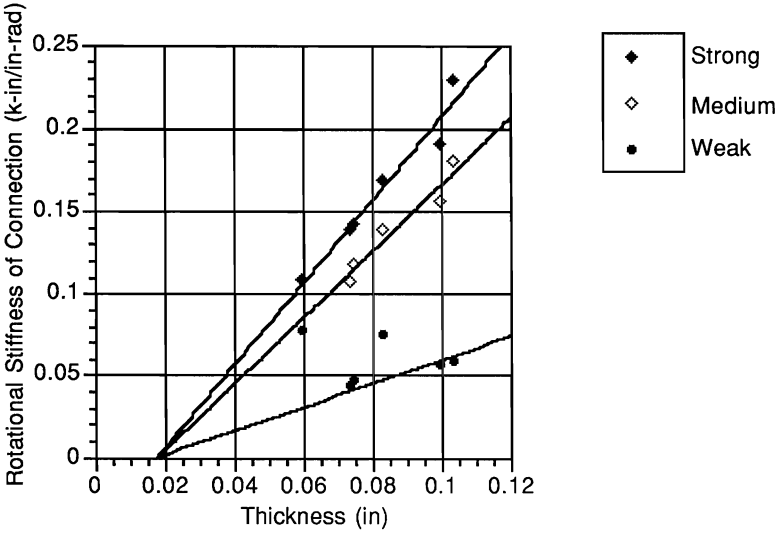


Fig. 4 Rotational Stiffness of the Deck to Flange Connection vs. Thickness

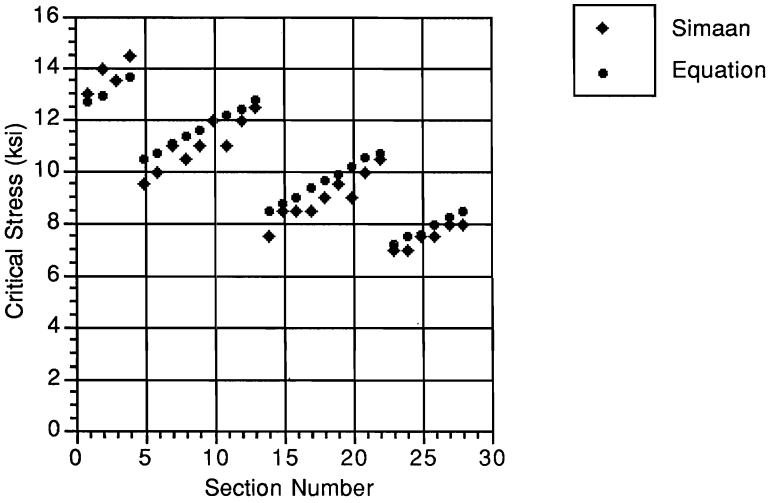


Fig.5 Equation (23) vs. Simaan -Z Sections ,Weak Fastener Location

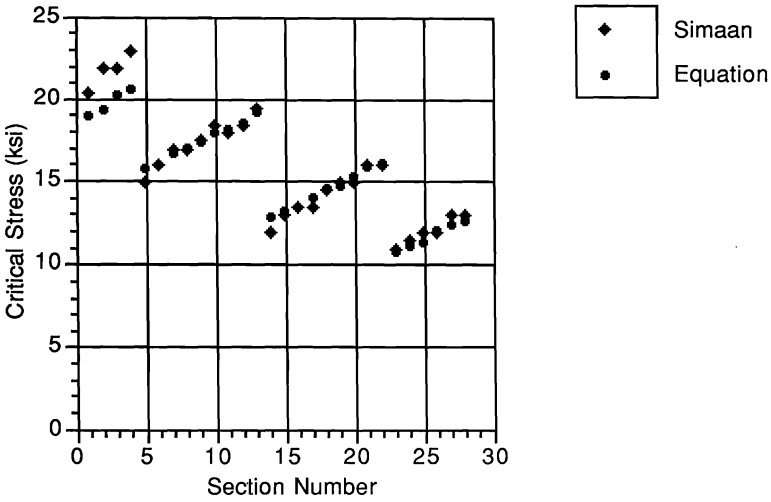


Fig.6 Equation (23) vs. Simaan -Z Sections ,Medium Fastener Location

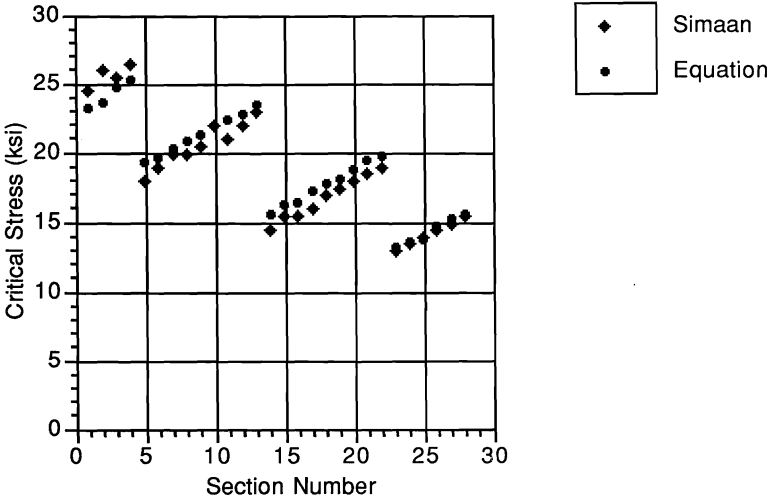


Fig. 7 Equation (23) vs. Simaan -Z Sections ,Strong Fastener Location

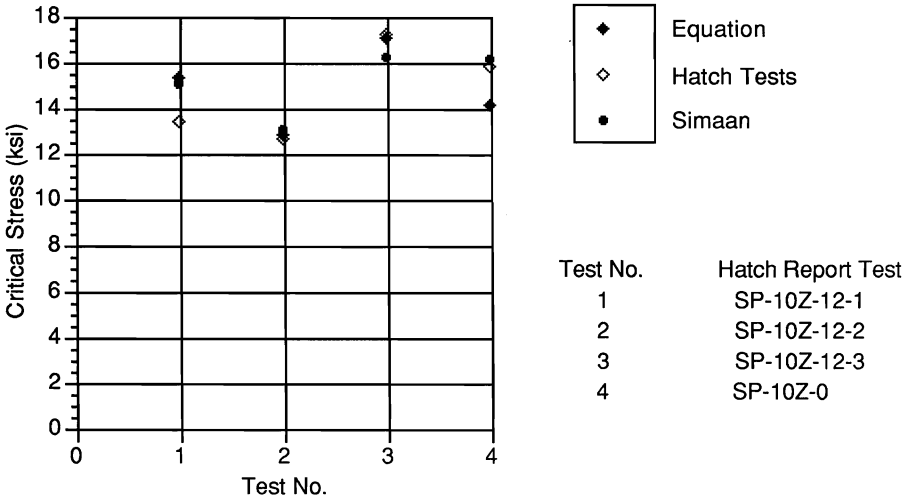


Fig. 8 Equation (23) vs Z Section Test Values

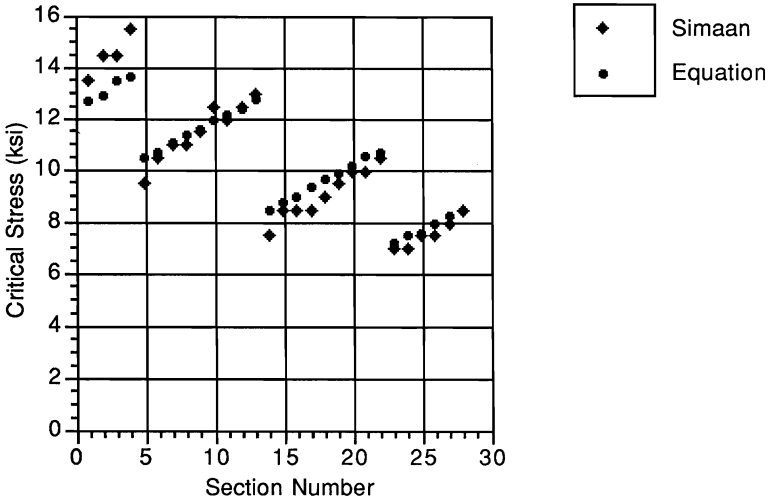


Fig.9 Equation (23) vs. Simaan -C Sections ,Weak Fastener Location

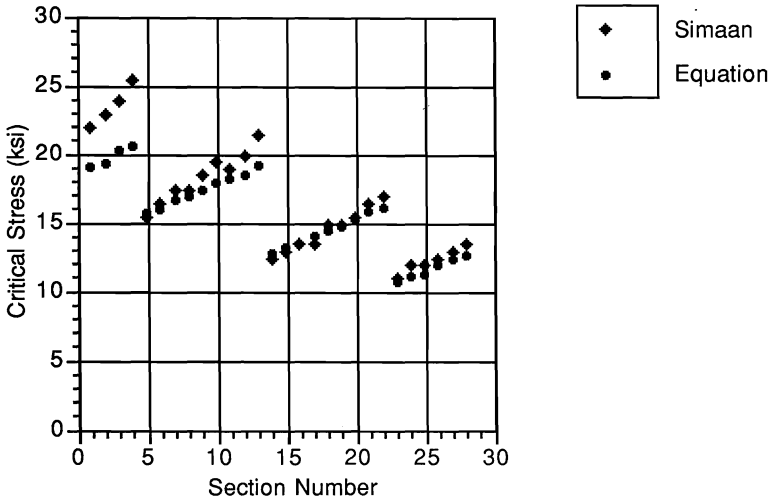


Fig.10 Equation (23) vs. Simaan -C Sections , Medium Fastener Location

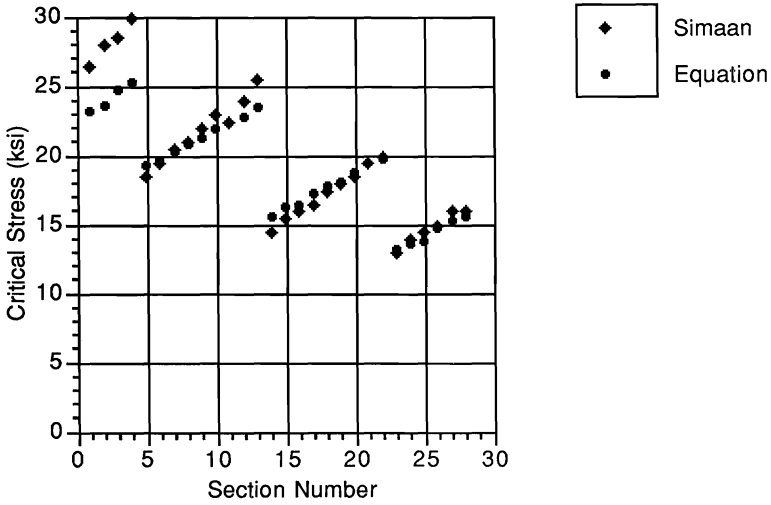


Fig.11 Equation (23) vs. Simaan -C Sections , Strong Fastener Location

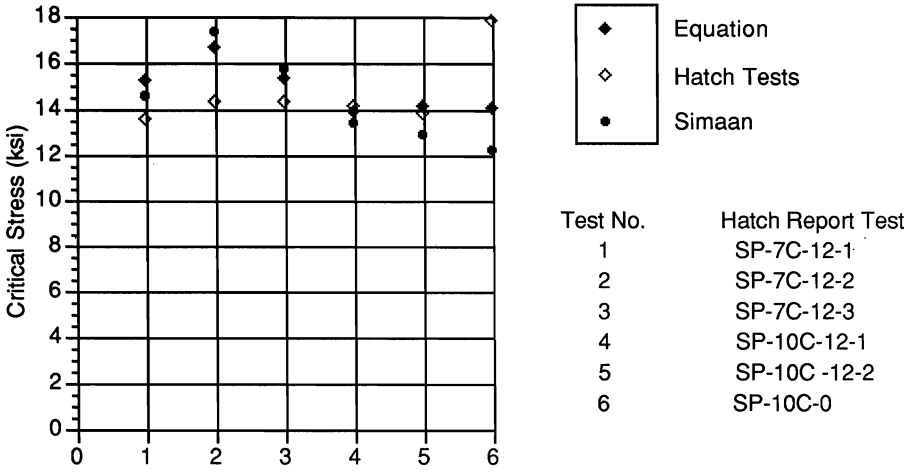


Fig. 12 Equation (23) vs. C Section Test Values

